

Title	Electromechanical coupling factors of single-domain 0.67Pb(Mg _{1/3} Nb _{2/3})O ₃ -0.33 PbTiO ₃ single-crystal thin films
Author(s)	Wasa, K; Ito, S; Nakamura, K; Matsunaga, T; Kanno, I; Suzuki, T; Okino, H; Yamamoto, T; Seo, SH; Noh, DY
Citation	APPLIED PHYSICS LETTERS (2006), 88(12)
Issue Date	2006-03-20
URL	http://hdl.handle.net/2433/50133
Right	Copyright 2006 American Institute of Physics. This article may be downloaded for personal use only. Any other use requires prior permission of the author and the American Institute of Physics.
Type	Journal Article
Textversion	none; publisher

Electromechanical coupling factors of single-domain $0.67\text{Pb}(\text{Mg}_{1/3}\text{Nb}_{2/3})\text{O}_3-0.33\text{PbTiO}_3$ single-crystal thin films

K. Wasa^{a)}*Faculty of Science, Yokohama City University, Yokohama, Japan*

S. Ito and K. Nakamura

Faculty of Electrical Engineering, Tohoku University, Sendai, Japan

T. Matsunaga

Matsushita Techno-Research, Osaka, Japan

I. Kanno and T. Suzuki

Faculty of Mechanical Engineering, Kyoto University, Kyoto, Japan

H. Okino and T. Yamamoto

The National Defense Academy, Yokosuka, Japan

S. H. Seo and D. Y. Noh

Kwangju Institute of Science and Technology, Kwangju, Korea

(Received 22 July 2005; accepted 26 February 2006; published online 21 March 2006)

Thin films of single *c*-domain/single-crystal $(1-x)\text{Pb}(\text{Mg}_{1/3}\text{Nb}_{2/3})\text{O}_3-x\text{PbTiO}_3$ (PMN-PT) with $x \cong 0.33$ near a morphotropic boundary composition were heteroepitaxially grown on (110)SRO/(001)Pt/(001)MgO substrates. The heteroepitaxial growth was achieved by rf-magnetron sputtering at the substrate temperature of 600 °C. After the sputtering deposition, the substrates were rapidly cooled from 600 °C to room temperature by atmospheric air gas at a cooling rate of 100 °C/min. The rapid cooling process enhanced the heteroepitaxial growth of the single *c*-domain/single crystal PMN-PT thin films. Their electromechanical coupling factor k_t measured by a resonance spectrum method was 45% at resonant frequency of 1.3 GHz with phase velocity of 5500 to 6000 m/s for the film thickness of 2.3 μm . The d_{33} and d_{31} were 194 pC/N and -104 pC/N, respectively. The observed k_t , d_{33} , and d_{31} were almost the same to the bulk single-crystal values. The present PMN-PT thin films are applicable for a fabrication of GHz planar bulk acoustic wave transducers. © 2006 American Institute of Physics. [DOI: 10.1063/1.2188588]

Relaxor based ferroelectric single crystal $(1-x)\text{Pb}(\text{Mg}_{1/3}\text{Nb}_{2/3})\text{O}_3-x\text{PbTiO}_3$ (PMN-PT) exhibits an exceptionally high piezoelectric constants with a high electromechanical coupling factor at the morphotropic phase boundary (MPB) around $x \cong 0.35$.^{1,2} Thin films of PMN-PT will be useful for a fabrication of thin film acoustic transducers, if the thin films exhibit the high k_t and/or high piezoelectric constants similar to the bulk PMN-PT single crystals. Several deposition processes of PMN-PT thin films were reported.³ Their piezoelectric properties, such as d_{33} and d_{31} were evaluated. The piezoelectric coefficients were mostly smaller than bulk values $d_{33}=2000$ pC/N, although relatively high values $d_{33}=1200$ pC/N were recently reported at a trench structure.⁴ The k_t of PMN-PT thin films in a GHz range has been not evaluated, although the evaluation of k_t in a GHz range is essential for a fabrication of GHz acoustic devices. The differences in the electromechanical coupling and/or piezoelectric properties between the bulk and thin films are not well understood, since these PMN-PT thin films included a dislocated interfacial layer.^{5,6} For a better understanding of the ferroelectric behavior of the PMN-PT thin films, the deposition of a single-domain/single-crystal structure without the interfacial layer is essential. This letter describes the deposition of single *c*-domain/single-crystal PMN-PT thin films with $x \cong 0.33$ (0.67PMN-0.33PT)

near the MPB composition and discusses their electromechanical coupling factor k_t measured in a GHz range in relation to their piezoelectric constants d_{33} and d_{31} .

A planar rf-magnetron sputtering system was used for the deposition of 0.67PMN-0.33PT thin films. The sputtering system was described in a previous report.⁷ 4-in. powder target was used for the sputtering. The powder target was composed of a mixture of PbTiO_3 , PbO, MgO, Nb_2O_5 and TiO_2 powder packed in a stainless shallow tray. The chemical composition of the mixed powder was 10% PbO-rich 0.67PMN-0.33PT. The substrates were (001)Pt/(001)MgO with buffer layer of (110)SrRuO₄(SRO). A mixture of Ar and O₂ with ratio of 20 to 1 was introduced at 0.5 Pa, and rf power was set at 90 W. The substrate temperature was held at 600 °C during the deposition. After the deposition the substrates were rapidly cooled from growth temperature 600 °C to room temperature by a cooling gas of atmospheric air at 1 atm. The substrate holder with heating block was designed to have a small thermal capacity so that the substrates were easily cooled down by the air gas. The cooling rate was 100 °C/min. The growth rates of the sputtered films were 0.2 to 0.3 $\mu\text{m}/\text{h}$. Electron probe microanalyses suggested the chemical composition of the sputtered films was stoichiometric 0.67PMN-0.33PT. The thickness of the sputtered films was selected from 1 to 3 μm for the measurement of electromechanical coupling k_t and the piezoelectric constants.

^{a)}Electronic mail: kiyotkw@hi-ho.ne.jp

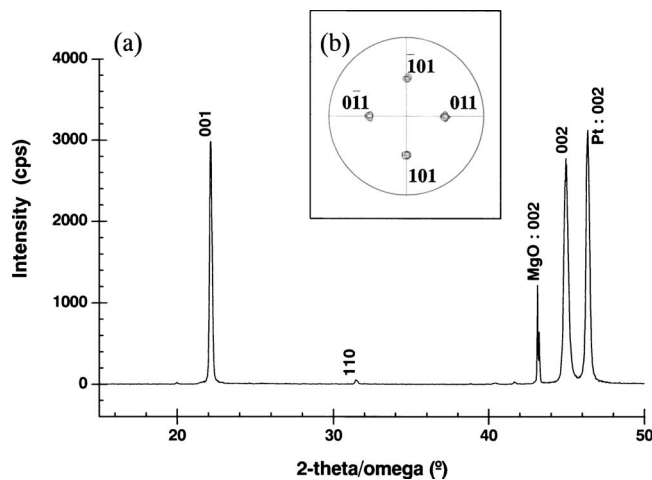


FIG. 1. Typical XRD patterns of the sputtered PMN-PT thin films with $x \cong 0.33$ near the MPB composition grown on (110)SRO/(001)Pt/(001)MgO substrates. (a) $\theta-2\theta$ pattern, (b) pole figures of (110) direction. Contours are drawn from 27 to 213 on a logarithmic scale (PMN-PT film thickness: $2.3 \mu\text{m}$).

Typical X-ray diffraction (XRD) patterns of the sputtered 0.67PMN–0.33PT thin films near the MPB composition were shown in Fig. 1. The XRD $\theta-2\theta$ pattern showed the sputtered film was highly (001) oriented PMN-PT structure [Fig. 1(a)]. The pole figure of (110) direction showed a strong four-fold intensity describing three-dimensional epitaxy, i.e., single-crystal structure [Fig. 1(b)]. The XRD analyses suggested the lattice parameters of the PMN-PT thin films at room temperature were $a=0.401_9 \text{ nm}$, $b=0.401_3 \text{ nm}$, $c=0.404_9 \text{ nm}$, $\alpha=90.00^\circ$, $\gamma=90.02^\circ$, $\beta=89.79^\circ$. These lattice constants were obtained by measuring the four-circle diffraction angles of 17 peaks different from each other. The possible crystal structure of the present PMN-PT thin films is a tetragonal structure with $a=b \cong 0.401 \text{ nm}$, $c \cong 0.405 \text{ nm}$, and $\alpha=\beta=\gamma \cong 90.00^\circ$. The room-temperature crystal phase of bulk PMN-PT near the MPB composition is rhombohedral and/or a mixture of rhombohedral and tetragonal phase.¹ The crystal structure of the PMN-PT thin films were modified from the bulk structure, if the PMN-PT thin films truly comprised the tetragonal structure. However, the in-plane lattice parameters of the PMN-PT thin films were almost the same to those of the bulk tetragonal phase and/or rhombohedral phase, i.e., $a_T=0.401_8 \text{ nm}$, $b_T=0.401_8 \text{ nm}$, $c_T=0.404_1 \text{ nm}$, $a_R \cong 0.402_3 \text{ nm}$, and $\alpha_R \cong 89.91^\circ$.¹ This indicates the PMN-PT thin films are almost free from in-plane stress. It is known the heteroepitaxial thin films of thickness thicker than $1 \mu\text{m}$ often comprise thick dislocated interfacial layer.^{8,9} However, cross-sectional scanning (SEM) and transmission electron microscopy (TEM) images of the present PMN-PT thin films showed that the PMN-PT thin films exhibited continuous structure without remarkable dislocated interfacial layer, although point defects were observed at the interface between the film and the substrates.¹⁰ The growth of the dislocated interfacial layer was possibly suppressed by the rapid cooling process.

The k_t and the d_{31} and d_{33} were measured for the present 0.67PMN–0.33PT thin films. The experimental values were compared with the 0.67PMN–0.33PT single crystal values.^{11,12} In order to evaluate the k_t , two ports planar bulk acoustic wave (BAW) resonator was fabricated using the

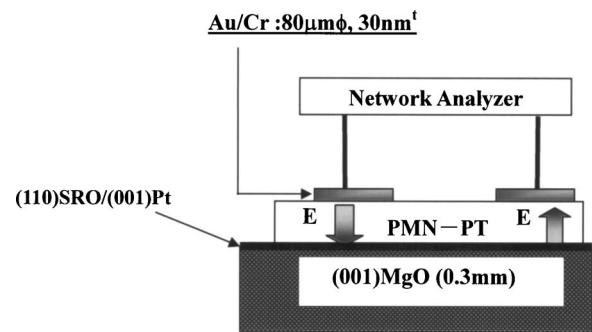


FIG. 2. Schematic construction of planar type two ports PMN-PT thin-film resonator.

PMN-PT thin films. The construction of the resonator is shown in Fig. 2. The k_t was evaluated by the resonance spectrum method recently developed for the evaluation of the BaTiO₃ thin films.¹³ A pair of vacuum evaporated Au/Cr input and output electrodes of $80 \mu\text{m}$ in diameter were formed on the surface of the PMN-PT thin films. The SRO/Pt layer was common earth electrode. The spacing between the two electrodes was $60 \mu\text{m}$. The resonator was composed of a pair of thin film resonator connected in series connection. The thickness of the PMN-PT thin films and MgO substrates were $2.3 \mu\text{m}$ and $300 \mu\text{m}$, respectively. The resonance spectra were measured across the electrodes by a network analyzer (HP-8719D). Typical resonance properties were shown in Fig. 3. The fundamental resonance signal was observed at about 1.3 GHz [Fig. 3(a)]. The multi-reflection mode is superposed on the main resonant signals [Fig. 3(b)]. The multi-reflection mode was caused by the acoustic multireflection of a longitudinal standing wave excited in the MgO substrate. The frequency of multireflection mode Δf is expressed by $\Delta f = v_{p\text{MGO}}/2d$, where $v_{p\text{MGO}}$ denotes the phase

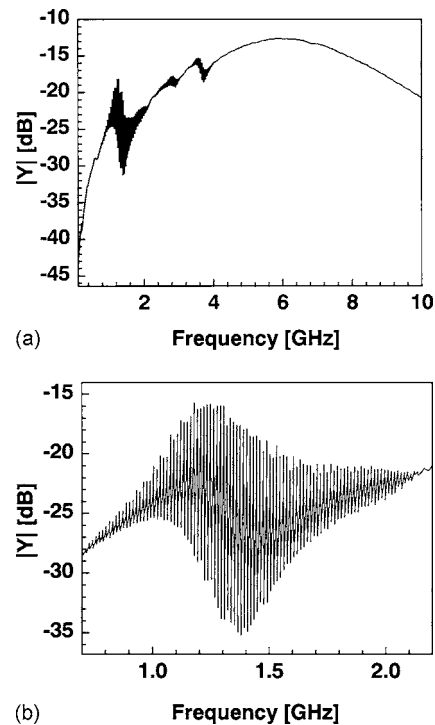


FIG. 3. Resonant properties of planar type two ports PMN-PT thin film resonator with $x \cong 0.33$ near the MPB composition for a different frequency range. (a) 0–10 GHz, (b) 0.7–2.2 GHz (PMN-PT film thickness, $2.3 \mu\text{m}$).

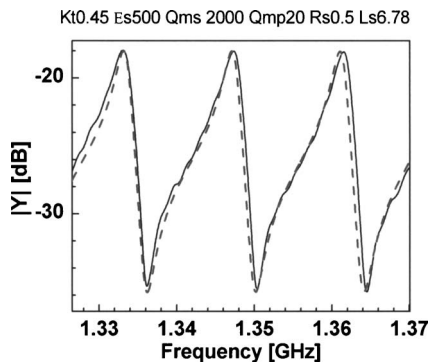


FIG. 4. Resonant properties of planar type two ports PMN-PT thin film resonator with a fitting curve analyzed by Mason's equivalent circuit at $\epsilon_{33}^s=500$ and $k_t=45\%$ with, $Q_{ms}=2000$, and $Q_{mp}=20$; solid line, measured curve; broken line, fitting curve (PMN-PT film thickness, $2.3 \mu\text{m}$).

velocity of longitudinal wave in the MgO and d denotes the thickness of the MgO substrates. Taking $v_{p\text{MgO}}=9000 \text{ m/s}$ and $d=300 \mu\text{m}$, Δf becomes 15 MHz . The k_t was calculated from the resonance properties using the Mason's equivalent circuits considering a propagation loss similar to the case of BaTiO₃ thin films. The analyses were done by the fitting of the equivalent circuit model with the observed admittance spectra. The typical fitting curve was shown in Fig. 4. From the fitting analyses the k_t was found to be 45% at resonance frequency of 1.3 GHz with $\epsilon_{33}^s=500$, $Q_{ms}=2000$, and $Q_{mp}=20$, where ϵ_{33}^s , Q_{ms} , and Q_{mp} were dielectric constant of PMN-PT thin films, mechanical Q values of substrates, and mechanical Q values of PMN-PT thin films, respectively. The phase velocity v_p of the longitudinal mode for PMN-PT thin films was 5500 to 6000 m/s . It is interesting the observed k_t and the phase velocity were close to the bulk values, $k_t=47\%$, $v_p=5232 \text{ m/s}$ for $0.67\text{PMN}-0.33\text{PT}$ single c -domain/single crystals near the MPB composition.¹¹ The d_{31} and d_{33} were evaluated by the deflection of cantilever beam and the inverse piezoelectricity using AFM stylus, respectively. The d_{31} is given by $d_{31}=e_{31}/Y_{\text{FILM}}$, where Y_{FILM} is Young's modulus of PMN-PT thin films. The PMN-PT thin films at MPB composition of $2.3 \mu\text{m}$ in film thickness showed $e_{31}=-5 \text{ C/cm}^2$ at the electric field less than 1 MV/m . Taking $Y_{\text{FILM}}=48 \text{ GPa}$,⁵ the d_{31} values became -104 pC/N . The d_{33} was evaluated with the Au/Cr top electrodes of 20 to $40 \mu\text{m}$ in diameter. The observed value of d_{33} , $(d_{33})_{\text{ob}}$, was around 70 pC/N . The $(d_{33})_{\text{ob}}$ is affected by the in-plane displacement. The effect of the in-plane displacement is corrected by the relation, $d_{33}=(d_{33})_{\text{ob}}-2[d_{31}s_{13}^E/(s_{11}^E+s_{12}^E)]$, where s_{13}^E , s_{11}^E , and s_{12}^E denote the mechanical compliances of the PMN-PT.¹⁴ Taking $d_{31}=-104 \text{ pC/N}$ and $s_{13}^E=-5.58 \times 10^{-12} \text{ m}^2/\text{N}$, $s_{11}^E=62.16 \times 10^{-12} \text{ m}^2/\text{N}$, and $s_{12}^E=-53.85 \times 10^{-12} \text{ m}^2/\text{N}$,¹¹ the d_{33} became 194 pC/N . These piezoelectric constants are also al-

most the same to the bulk single domain/single crystal values, $d_{31}=-90 \text{ pC/N}$, $d_{33}=190 \text{ pC/N}$. The measurements included errors, since bulk elastic constants were used for the calculation of d_{33} and d_{31} . In contrast, the measurement of the k_t is less obscure. It is clear the k_t measured in a GHz range is almost the same to the bulk single crystal, 95% of bulk single-domain/single crystals, although the PMN-PT thin films show the tetragonal structure contrary to bulk rhombohedral structure.

Synchrotron scattering XRD analyses of the PMN thin films suggest the sputtered PMN thin films under the present rapid cooling process comprise the B-site chemical ordered nanoregion that is suggested as an origin of relaxor behavior.¹⁵ The high electromechanical coupling observed in the present PMN-PT thin films may be also owed to the presence of the B-site chemical ordered nanoregion similar to the PMN thin films.

In conclusion single c -domain/single crystal $0.67\text{PMN}-0.33\text{PT}$ thin films near the MPB composition were fabricated by magnetron sputtering under rapid cooling process. Their piezoelectric constant and electromechanical coupling factor k_t were almost the same to the bulk single-domain single crystals. The k_t in a GHz range was found to be 45% . The present PMN-PT thin films have high potential in the fabrication of GHz BAW transducers and/or GHz planar resonator.

The authors thank H. Harada and Professor H. Kotera (Kyoto University) for their measurements of piezoelectric properties and useful discussion.

- ¹O. Noblanc, P. Gaucher, and G. Calvarin, *J. Appl. Phys.* **79**, 4291 (1996).
- ²K. Uchino, *Solid State Ionics* **108**, 43 (1998).
- ³K. Wasa, M. Kitabatake, and H. Adachi, *Thin Film Materials Technology* (Springer, William Andrew Pub., New York, 2004), p. 405.
- ⁴D. M. Kim, C. B. Eom, J. Quyang, V. Nagarajan, R. Ramesh, V. Vaithyanathan, D. G. Schlom, W. Tian, and X. Q. Pan, *Abstract, 2004 IEEE International Ultrasonic, Ferroelectrics, and Frequency Control Joint Conference* (IEEE, Montréal, 2004), p. 58.
- ⁵J. H. Park, F. Xu, and S. Trolier-McKinstry, *J. Appl. Phys.* **89**, 568 (2001).
- ⁶Z. Kighelman, D. Damjanovic, and N. Setter, *J. Appl. Phys.* **89**, 1393 (2001).
- ⁷K. Wasa, Y. Yamada, M. Shimoda, S. H. Seo, D. Y. Noh, H. Okino, and T. Yamamoto, *Proceedings of 13th IEEE International Symposium on Applications of Ferroelectrics* (IEEE, Nara, 2002), p. 179.
- ⁸C. M. Foster, W. Pompe, A. C. Daykin, and J. S. Speck, *J. Appl. Phys.* **79**, 1405 (1996).
- ⁹R. Ai, H. Itoh, G. Asayama, and K. Wasa, *Proc. SPIE* **4058**, 426 (2000).
- ¹⁰S. H. Seo, PhD thesis (Kwangjyu Institute of Science and Technology, Kwangjyu, 2004), p. 88.
- ¹¹R. Zhang and W. Cao, *Appl. Phys. Lett.* **85**, 6380 (2004).
- ¹²R. Zhang, B. Jiang, and W. Cao, *Appl. Phys. Lett.* **90**, 3471 (2001).
- ¹³S. Ito, K. Nakamura, and K. Ishikawa, *Proceedings of 2005 IEEE International Ultrasonics Symposium* (IEEE, Rotterdam, 2005), p. 1L-7.
- ¹⁴K. Lefki, and G. J. M. Dormans, *J. Appl. Phys.* **76**, 1764 (1994).
- ¹⁵S. H. Seo, H. C. Kang, Y. Yamada, K. Wasa, and D. Y. Noh, *Appl. Phys. Lett.* **84**, 3133 (2004).